ISSN 0016-8521, Geotectonics, 2020, Vol. 54, No. 6, pp. 785–796. © Pleiades Publishing, Inc., 2020.
Russian Text © The Author(s), 2020, published in Geotektonika, 2020, No. 6, pp. 77–90.

Identification of Ruptures and their Interaction with Hydrothermal–Magmatic Systems on Northern Paramushir Isl. (Kuril Islands, Russia): 3D Modeling of Tectonic Fragmentation

O. R. Khubaeva[a, b, *], O. V. Bergal-Kuvikas[a–c], and M. D. Sidorov[d]

[a] *Institute of Volcanology and Seismology, Far East Branch, Russian Academy of Sciences, Petropavlovsk-Kamchatsky, 683006 Russia*

[b] *Schmidt Institute of Physics of the Earth, Russian Academy of Sciences, Moscow, 123242 Russia*

[c] *Institute of Geology of Ore Deposits, Petrography, Mineralogy, and Geochemistry, Moscow, 119017 Russia*

[d] *Scientific Research Geotechnological Center, Far East Branch, Russian Academy of Sciences, Petropavlovsk-Kamchatsky, 683002 Russia*

**e-mail: grifon03@yandex.ru*

Received April 13, 2020; revised July 12, 2020; accepted July 28, 2020

Abstract—Correlation of ruptures with volcanic activities, and related hydrothermal-magmatic systems are studied. In our research we used a set of methods that included analysis of satellite data, identification lineaments and voxel modeling of crustal fragmentations. The main geological structure that ensures transportation of thermal energy in the hydrothermal-magmatic systems in the northern part of Paramushir Isl., and the a sill-dike complex associated with the system of north-eastern and sub-latitudinal fractures is considered. The formation of the northeast oriented ruptures is perpendicular to stretch of the submerged plate and reflects the stress regime in the island-arc setting. In the north of Paramushir Isl. ruptures with sub-latitudinal directions are recorded. The ruptures are located on the extension of the regional fault which is perpendicular to the main axis of the back-arc Kuril basin.

Keywords: lineament, fracture, crustal fragmentation, intrusion, hydrothermal–magmatic systems

DOI: 10.1134/S0016852120060072

INTRODUCTION

Contemporary volcanic activity and associated hydrothermal activity on the Paramushir Isl. is associated swarms of dikes that trace faults and are the main heat sources for hydrothermal systems.

The location of side, monogenic cones on volcanoes and subvolcanic intrusions is controlled by the manifestation of regional stress fields [36, 37, 42, 47]. At convergent plate boundaries, at the front of island arcs, compression settings generated by the activity of back-arc basins most often predominate [41]. In the last decade, a technology that synthesizes the results from deciphering aerial photographs and voxel modeling was developed [24, 25, 44]. That technology made possible to assess the degree of fragmentation of the crust, as well as to trace its relationship with ore-magmatic, hydrothermal, and volcanic systems.

The comprehensive analysis of the spatial position of volcanoes of the Kuril Island arc was first carried out by G.P. Avdeiko et al. [1]. A characteristic feature of volcanoes is their localization in chains, obliquely, at different angles oriented relative to the general trend of the arc [1]. However location of volcanoes is not random and is largely controlled by regional stress in the crust [1, 4, 24, 25, 36, 37, 44, 47]. The aim of the article is to identify faults and study their relationship with volcanism and hydrothermal–magmatic systems.

GEOLOGICAL AND GEOMORPHOLOGICAL CHARACTERISTICS OF THE STUDY REGION

The Kuril Island arc (Fig. 1) is a classical subduction system. Within the arc, 36 active terrestrial and 116 submarine Quaternary volcanoes have been identified [1, 4]. Hydrothermal–magmatic activity is manifested at seven volcanoes (Ebeko, Sinarka, Kuntominar, Chirinkotan, Palass, Berg, Kudryavy, Tyatya, and Mendeleev) and on six islands (Paramushir, Shiashkotan, Chirinkotan, Ketoy, Utur, and Iturup) [45].

Within the Kuril Island arc, the most widespread are the Pliocene–Quaternary subduction (island arc) type of volcanic rock, their composition varies from basalt to rhyolite, but the proportions of rocks also varies in different segments of the arc. In general, basaltic andesite and andesite (60–70%) predominate [2, 3]. The Kuril Island arc is characterized by high modern tectonic and volcanic activity. The position of volca-

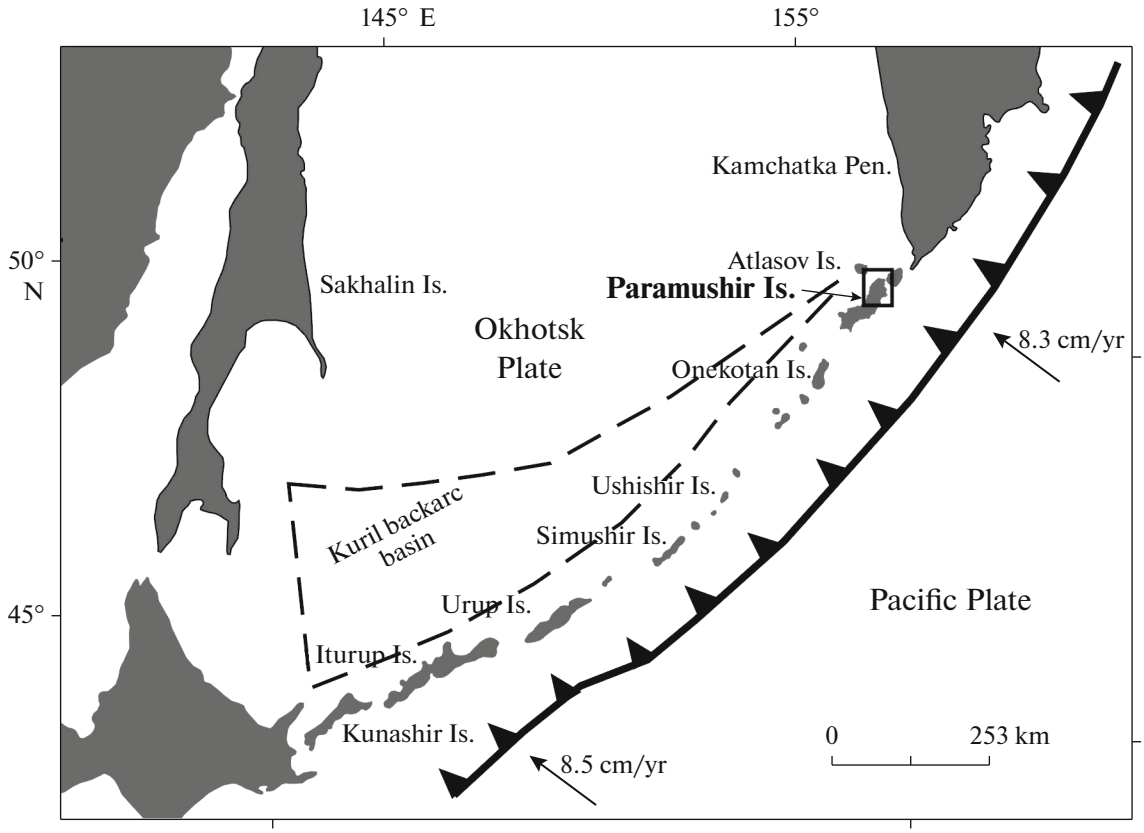

Fig. 1. Schematic map of the Kuril island arc.

noes and their composition are determined by the depth to the subducted plate and the distance from the volcanic front [1]. Based on concentration of volcanic centers across the arc, the front and rear volcanic zones with an intermediate area of attenuating volcanic activity have been distinguished [1].

Paramushir Isl. (see Fig. 1) is formed by the Neogene, mainly volcano-sedimentary rocks, crumpled into gently dipping folds, elongated along the trend of the island arc, which is not typical of other islands of the Greater Kuril arc [21]. The relief on Paramushir Isl. is distinguished by three volcanic ridges: the Vernadsky, Levinson-Lessing, and Karpinsky. The northern part of the island is made up of Upper Miocene–Pliocene, Quaternary, and modern rocks. The basement is consists of rocks of the Paramushir Isl. volcano-sedimentary complex. In the Pleistocene and Holocene, andesitic lava flows were formed in Vernadsky Ridge on southwestern Paramushir (volcanic group consisting of Chikurachiki, Tatarinova, Lomonosov, Fuss Peak volcanos) and the Ebeko volcanic group in the north [27]. According to I.V. Melekestsev [19], the age of eruptive centers localized along large NNE-trending linear zones (Karpinsky and Vernadsky ridges) has been established as 350–300 to 60–50 ka. For the youngest landforms, the Vernadsky Ridge (volcanic centers of the Ebeko volcanic group), the age has been determined as 2400–2500 years. Based on the localization of volcanism, microscopic description of rocks, and geochemical analysis, distinctive geological and petrological features of volcanogenic formations were established in three main zones of the Paramushir segment of the Kuril Island arc: the frontal, intermediate and rear zones. The formation of the distinguished tectonic zones of volcanic rocks across the trend of the arc depends on dehydration of the plate in the frontal zone and melting of sediments in the rear zone [32].

RESEARCH METHODS

To identify faults on the Earth's surface, a set of methods widely used in geology was applied. Deciphering of satellite and aerial photographs, together with lineament analysis, made it possible to identify zones of increased permeability to vapor–hydrothermal fluids; voxel modeling was used to identify tectonic destruction zones.

In order to determine zones permeable to vapor–hydrothermal fluids on northern Paramushir Isl., diagrams of lineament networks were constructed based on the deciphering of 1 : 50000 topographical map and aerial and satellite images of various detail. The distribution of lineaments reveals blind faults and the structure of the deep (bedrock) parts of hydrothermal–magmatic systems.

Deep-seated linear inhomogeneities in the structure of the crust are represented by (1) rises and riselike highs; (2) grabens and grabenlike lows; (3) increased fracture zones; (4) flexures and flexural-fault zones; (5) ruptures and faults with different occurrence depths; (6) linearly oriented fold belts; (7) zones of increased magmatic permeability; (8) chains of intrusive bodies, extinct and active volcanoes.

Along the extent, lineaments (local, regional, transregional) or super- and global (planetary) lineaments are observed [13]. Lineaments are often found in the ordering of the erosion network (erosional dissection of the Earth's surface), which makes it possible to interpret them as zones of weakness or permeable zones. The spatial distribution, as well as density and number of intersections of lineaments per unit area, are key factors for identifying highly permeable zones serving as migration routes for material [23].

3D MODELING OF TECTONIC FRAGMENTATION OF NORTHERN PARAMUSHIR ISL.

To construct a 3D model of tectonic fragmentation of northern Paramushir Isl., fracture tectonic maps were used, constructed from interpretation of aerial and satellite images of various levels of detail, as well as topographical maps of various scale.

Analog maps were digitally processed using GIS. Georeferencing and vectorization of the deciphering results were done in ArcMap [44] and ArcView [48]. Based on the vectorized data, a unified digital map of lineaments northern Paramushir Isl. was created.

The fragmentation of the geological setting can be quantitatively estimated from the specific length of lineaments [18]. The specific length of lineaments for identifying tectonic destruction zones is represented as a 3D matrix, from which a volumetric image of fragmentation of the investigated block is formed.

"Tectonic fragmentation" of a cubic block is determined from the ratio of the volume of all fractures within the block to its volume. The volume (V) of fractures is defined as the sum of the products of the length (l), opening width (b), and penetration depth (h) of individual fractures:

$$V = \Sigma lbh.$$

For a cubic block with edge a, in which one of the faces is the Earth's surface, the tectonic fragmentation coefficient is be

$$\Sigma lbh/a^3.$$

It is impossible from a photo image to determine the b and h values, but for a specific localized area, the fracture width b can be considered constant: $b = \text{const}$. Also, taking into account the empirically established rule that the fracture of one face of a cube of rock adequately reflects the degree of fracturing in the entire sample [18] and, based on similarity principles, this rule can be approximated for individual crustal blocks. Then the penetration depth of of fractures h can be taken equal to edge a. Thus, defining the degree of fragmentation as the value of the specific length of lineaments as equal to $\Sigma l/a^2$ of the upper face of the block and successively increasing the size of the unit cell (cube), it is possible to trace the fragmentation to depth.

Considering the rheological properties of the medium in the cell to be homogeneous, the values of the specific length of lineaments calculated in this way pertain to the center of the cube at depth $a/2$. The algorithm is described in detail in [22, 24, 25].

The model was constructed in several stages. First, a square grid with a cell size of 1 km^2 was superimposed on the lineament map; within each cell, the total length of lineaments was calculated and normalized to the area of the cell. The values obtained pertained to the centers of the cubes. The edge of each cube was 1 km in length. This is how the lineament specific length matrix was compiled for a depth of 0.5 km. Sea level was taken as the zero mark. Then a correction for the relief was introduced (the height of the center of the upper face of each elementary cube), since the upper face of each cube is on the Earth's surface.

At the next stage of calculations, the edge size of an elementary cube was increased by 200 m and the entire procedure was repeated. A study of fracturing was carried out successively to a depth of 3 km. The obtained data for all depth levels are combined into one 3D matrix (X, Y, Z and UDL), used for volumetric display. The specific length of the lineaments is expressed in km^{-1}. This dimension follows from the calculation formula (see above).

For the volumetric image, the standard Oasis Montaj module (Geosoft) is applied [49], but other programs that support 3D raster formats can be used.

A set of studies carried out on the geothermal systems of Vernadsky Ridge since 2003 to identify the ratio of magmatic and hydrothermal processes in zones of active volcanism with heat supply sources, places of their localization, and relationships with faults. Spatial referencing of individual intrusive bodies, explosion craters, and geothermal manifestations, as well as delineation of hydrothermally altered rocks, was carried out using GPS. The data obtained were edited, transferred to ArcGis [48], and combined with satellite images [50] and aerial photographs, as well as a topographical map at a scale of 1 : 50000.

To assess volcanic activity in the Kuril Island arc, including Paramushir Isl., calculations of the productivity of volcanoes and their spatial positions relative to a deep-water trench were used [8]. The authors' generalization of the data on faults on northern Paramushir, as well as observations of volcanic activity and the temperature regime of the island's hydrothermal systems, made it possible to assess the relationship between faults and manifestations of volcanic and hydrothermal–magmatic activity.

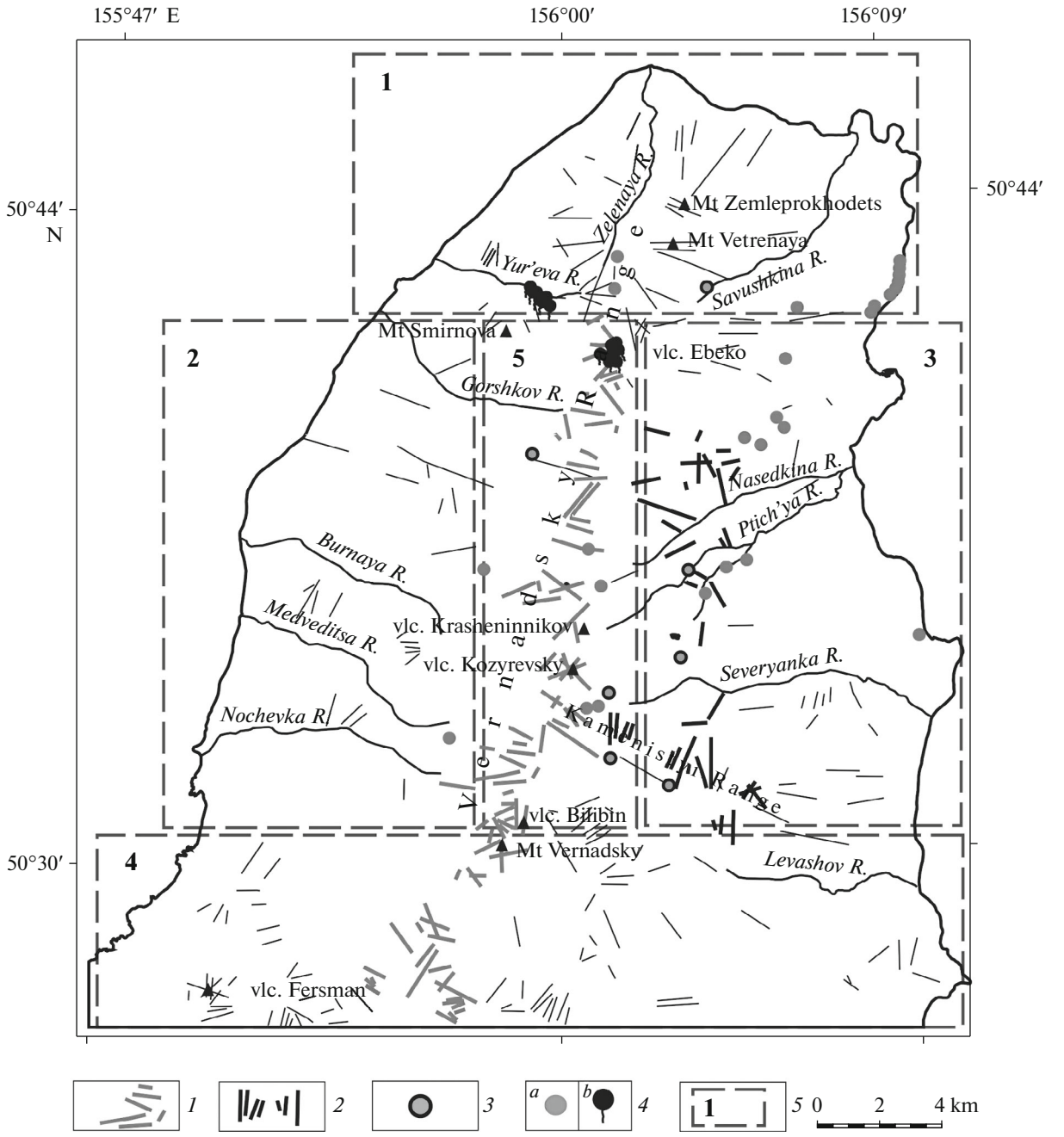

Fig. 2. Lineament network diagram for Paramushir Island. (*1*) Axial submeridional zone in lineament network diagram; (*2*) eastern permeability zone; (*3*) sources with limonite cones; (*4*) sources: (*a*) cold, (*b*) hot; (*5*) boundaries of sectors.

RESULTS OF IDENTIFYING FAULTS

To refine the permeable zones of the upper crust for the northern sector of Paramushir Isl., a lineament network diagram (Fig. 2) and 3D model of tectonic fragmentation of a block of rock were constructed. Based on the results of measuring the trend of the lineaments, diagrams of the trends of local tectonic fracture zones were plotted by sector (see Figs. 2, 3). The diagrams made it possible to establish general patterns in the trend of lineaments. The data obtained indicate that the NE trend of lineaments predominates in all sectors. However, in the northern segment, an additional sublatitudinal trend of faults is distinguished (see Fig. 3f).

A possible explanation for the predominant NE trend of lineaments is the effect of regional tectonic stress. Based on seismic data, earthquakes focal mechanisms, the nature of sedimentation, and the morphology of volcanic edifices in the Kuril Island arc, a compression setting predominates [30, 31]. Consequently, the revealed predominant NE trend of regional faults can be explained by the classical model

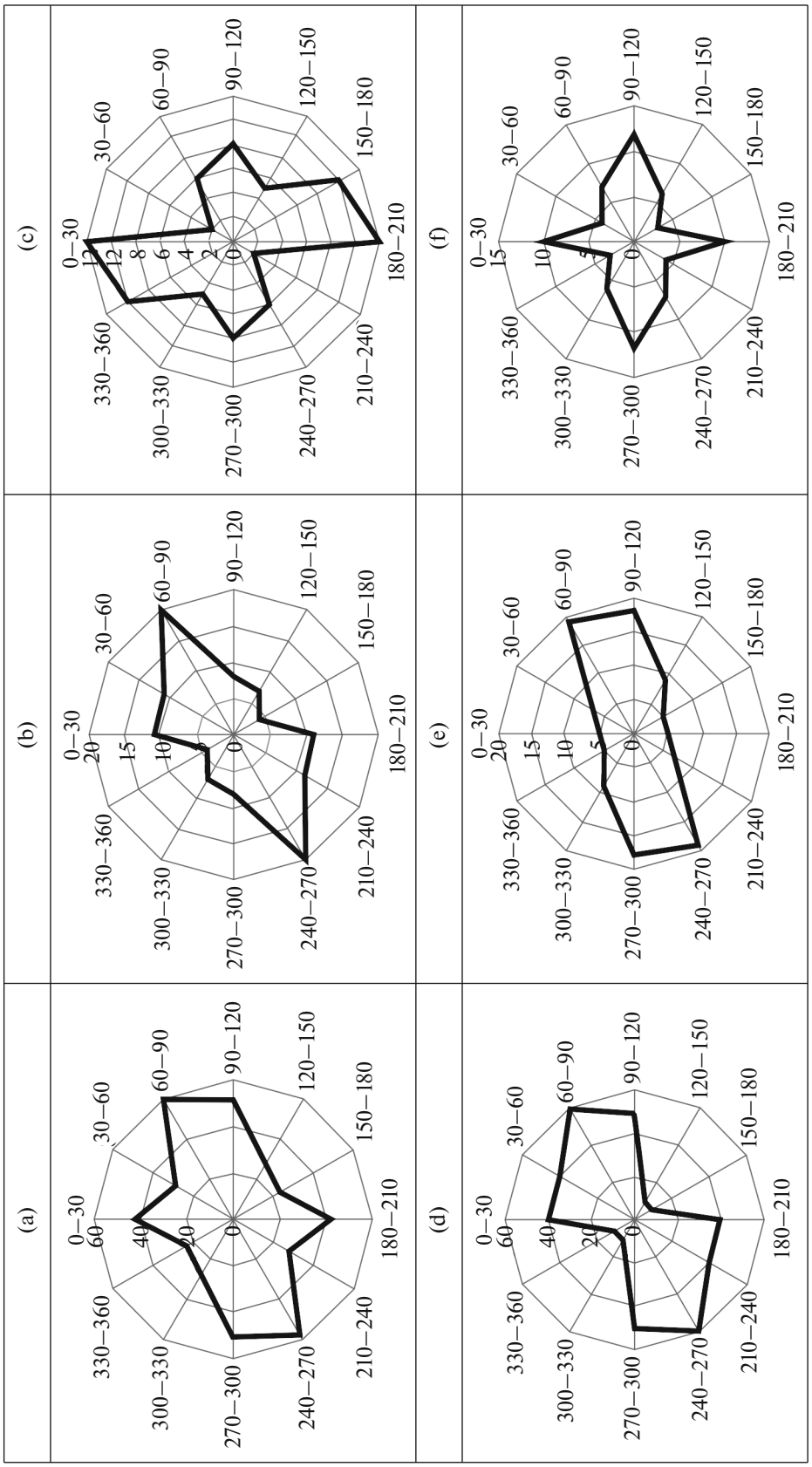

Fig. 3. Trends of tectonic fracture zones. (a) general diagram of trend of tectonic fracturing zones on northern Paramushir; (b)–(f) trend of tectonic fracturing zones in sectors: (b) southern, (c) eastern, (d) western, (e) central, (f) northern.

of formation of zones of weakness oriented perpendicular to the compression axis [40]. The data agree with factual material on the dominant NE-trending faults within the Kuril Island arc [12].

On northern Paramushir, both submeridional and sublatitudinal faults are distinguished [29]. Sublatitudinally trending faults have been noted by many authors. B.V. Baranov et al. [30] suggested that the numerous monogenic cones of the Alaid volcano, which strike NW–SE [27] mark the edge of the Kuril back-arc basin and are associated with sublatitudinally trending faults. It is possible that the back-arc basin dynamics extends to the rear Alaid volcanoes, the submarine Grigoriev volcano, and the front of the arc to Paramushir Isl.

Thus, the location of Paramushir Isl. in a compression setting and the back-arc basin dynamics form the main directions of faults.

DISCUSSION

Tectonic fracturing can propagate to great depths, forming paths for deep-circulating heated water flows to ascend to the Earth's surface. Also, increased tectonic fracture zones are indicators of fault zones and large faults. For example, modern volcanic and associated hydrothermal activity in Iceland, Hawaii, the Kuril Islands, as well as Kamchatka and North America, despite their different genesis, are often associated with a network of dikes [5, 11, 33, 35, 42], which are the main heat sources for hydrothermal systems.

On the lineament network diagram (see Fig. 2), as well as on the horizontal sections of the 3D model of tectonic fragmentation of a block of rock for northern Paramushir (Fig. 4), it can be seen that the greatest destruction is characteristic of the axial part of Vernadsky Ridge and its termini, to which all Late Pleistocene–Holocene volcanic activity is confined. The axial zone of areal volcanism reflects a fragmented sector of the crust, where the intrusion of dikes, forming a linear-nested type of volcanism, took place, after [10].

The productivity of monogenic volcanoes that formed in the Pliocene–Quaternary, located on NE-trending faults, varies from 3 to 7 km^3 [8], where a zone of high rock fragmentation is most clearly manifested (see Fig. 4) and all high-temperature sources and active fumarolic activity are concentrated. According to geological data [4], a NNE strike has been established in this area. On vertical sections of the 3D model of tectonic fragmentation (Figs. 5a–5c), destruction zones are well traced, extending to a depth of more than 3 km. Such zones are visible under volcanic edifices and apparently reflect the position of volcanic magmatic systems at depth.

In the axial part of Vernadsky Ridge, the ancient magma feeder systems (explosion craters, a system of basalt, basaltic andesite, and andesite dikes and necks) of the ancient Vetrovaya (present-day Zelenaya River valley), Vlodavets (present-day Yur'eva River valley) and Bogdanovich volcanoes (central zone of Vernadsky ridge) are partially exposed (Fig. 6). It is noteworthy that the subvolcanic bodies (necks and dikes) on northern Paramushir are associated with the distribution zones of hydrothermally altered rocks as a result of previously active hydrothermal activity (see Fig. 6) and coincide with clusters of anomalous rock fragmentation (see Fig. 4).

In contrast to the volcanoes confined to the NE-trending areal zone, Ebeko volcano, located at the intersection of NNE-, NE-, and NW-trending faults [29], has a volcanic edifice with a larger volume (~13 km^3) and higher frequency of fumarole and explosive activity during the historical observation period, in comparison to other volcanoes on northern Paramushir [7, 8]. The volcanic edifice is oriented relative to the main trends of the lineaments. Ebeko volcano is a cone with a relative height of 200–220 m (absolute elevation 1037 m), strongly elongated in the meridional direction with three contiguous craters at the summit, which are elongated in a chain from north to south [10]. The dimensions of the craters are approximately the same: (1) ridge diameter ~300–350 m; (2) bottom diameter ~200 m; (3) the total size of summit crater 350 × 800 m.

On the eastern and western slope of Ebeko volcano are two open amphitheaters, apparently representing adventive explosion craters, strongly widened by erosion. The same smaller crater with a small lake exists on the northern slope of Ebeko volcano [10]. Based on lithological, mineralogical, and petrographic studies of crater–lacustrine deposits, G.G. Khramova [28] demonstrated that the volcano is characterized by alternating periods of dormancy with the accumulation of sulfur–opaline deposits and phreatic and phreatomagmatic activity. Six stages of increased activity of Ebeko volcano have been distinguished, lasting 200–300 years, separated by periods of relative quiescence with the same duration. It was established that the eruption of juvenile material (lavas and pyroclastics) occurred only at stage I (420–200 BCE). Based on historical information supplemented by tephrochronological studies, it was revealed that all eruptions were phreatic and conditionally phreatomagmatic with a heat supply source in the form of a dike–sill complex with a volume >1 km [16, 17]. Finds of lava bombs like "bread crust" near active craters, may indicate the emplacement of mafic material into the volcanic edifice and the formation of phreatomagmatic activity [39]. Low-temperature, HCl, S (pH < 1) gas–hydrothermal fluids of Ebeko volcano are localized in the Northeast and South fumarole fields, crater lakes, and springs in the upper reaches of the Lagernyi Creek [9, 34]. A distinctive feature of gas–hydrothermal fluids is the variability in the composition and localization of outcrops [15]. Thus, during the observation period of 1963–1985, the variation in temperatures,

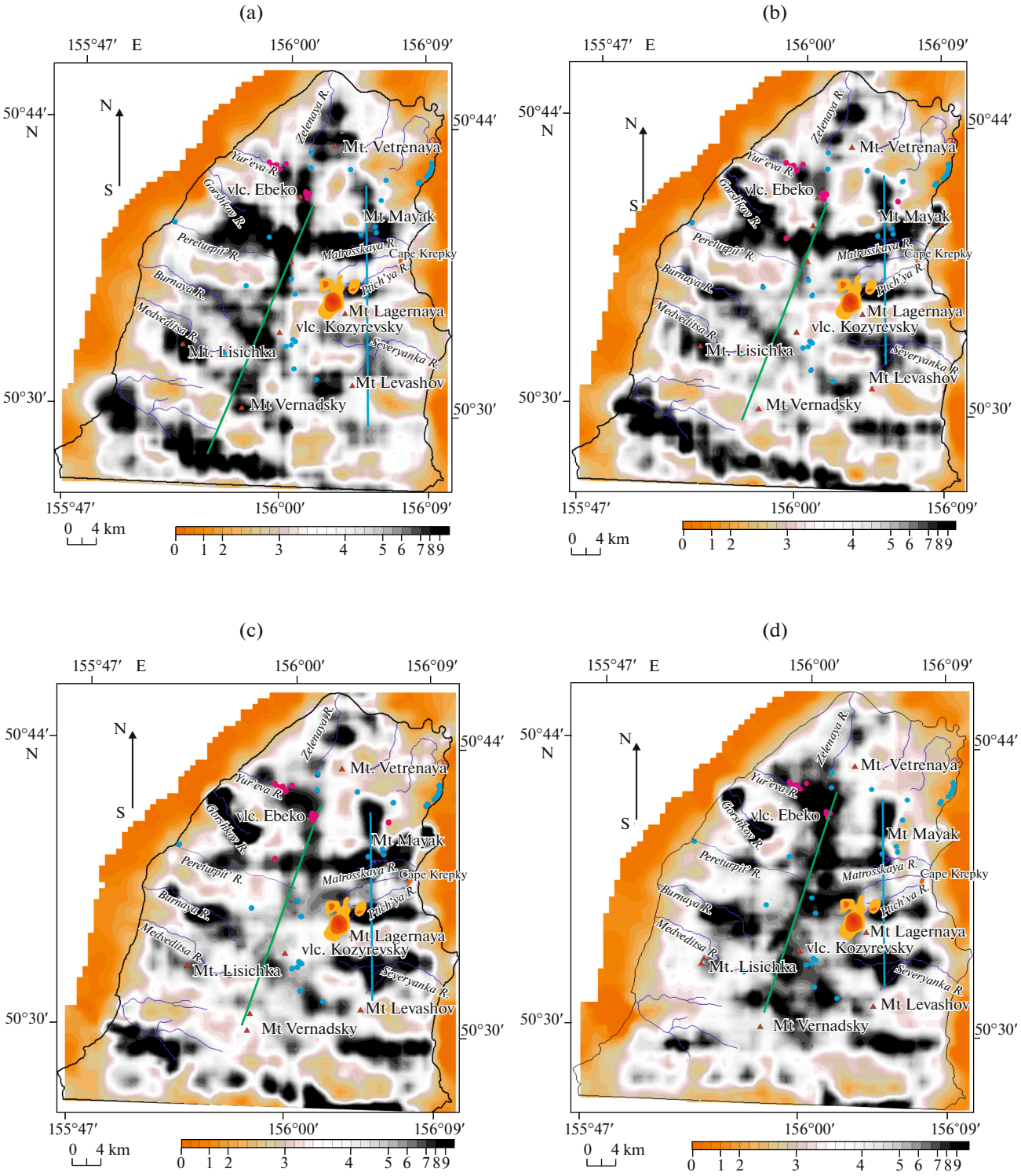

Fig. 4. Horizontal sections from 3D tectonic fragmentation model of block' rock for northern Paramushir at depths of study. Section at depth: (a) sea level 0.5 km below sea level; (b) 1 km below sea level; (c) 1.5 km below sea level; (d) 2 km below sea level. The distribution of specific lengths of lineaments (SLL) (km^{-1}) is shown. Green line denotes axial zone of Vernadsky ridge; blue line, blind fault on eastern slope of Vernadsky ridge; dots, sources: cold (blue); thermal (red); orange and tellow tones, intrusive bodies on Ptich'ya River.

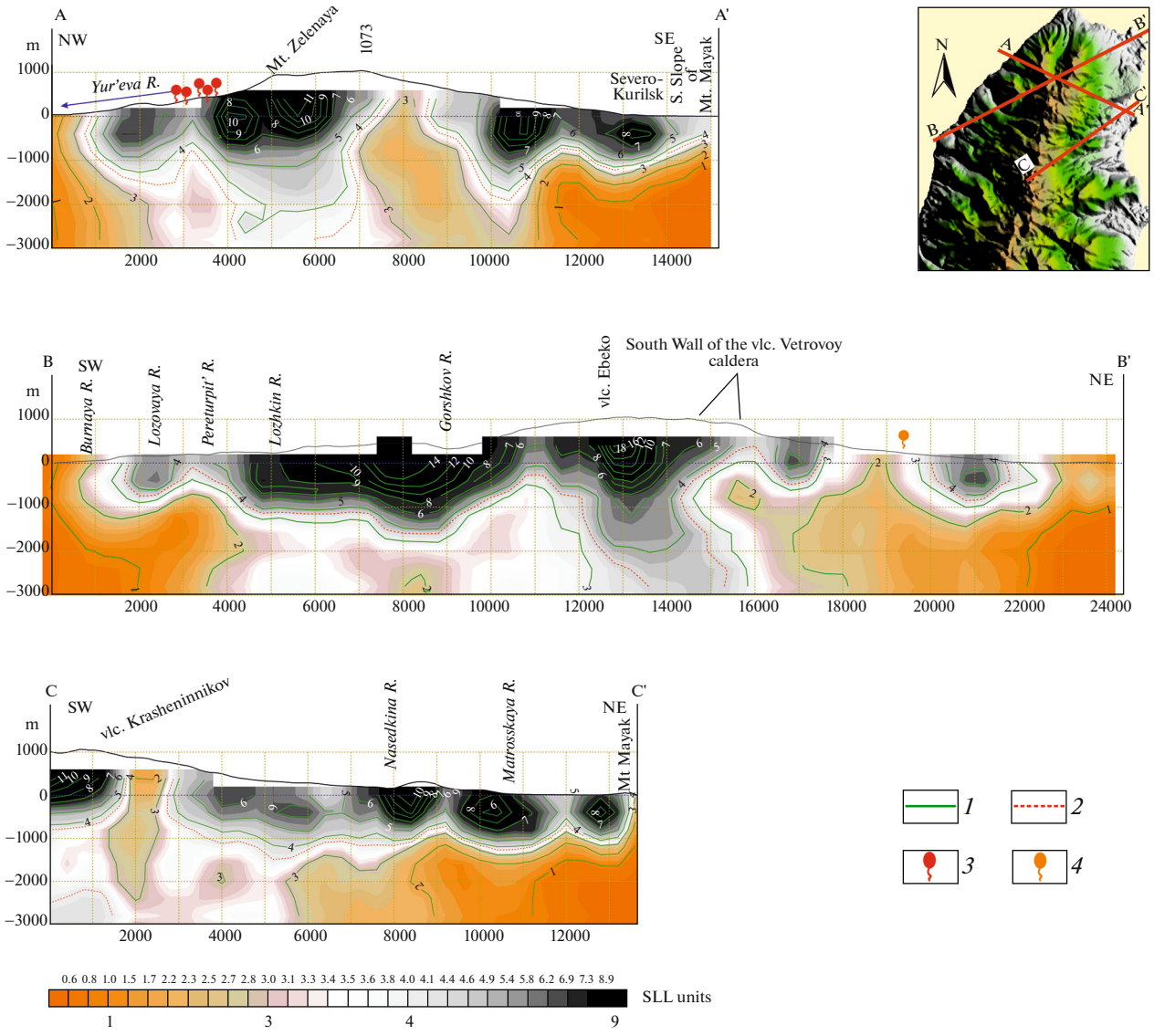

Fig. 5. Vertical sections of 3D tectonic fragmentation model for northern Paramushir for lines A–A', B–B', C–C'. Lines A–A', B–B', B–C' denote sections shown in figure. (*1*) SLL isolines, km^{-1}; (*2*) SLL of average (background) fragmentation on northern Paramushir; (*3*) high-temperature thermal springs; (*4*) highly mineralized springs with temperature of 11–24°C.

variations in the contents of H_2O/CO_2, CO_2/H_2, S/C, F/Cl, and S/Cl made it possible to identify the periods of activation and preparation for the phreatomagmatic eruptions of 1967 [39] and 2010–2011 [14].

The active effect of sublatitudinal faults is manifested in the formation of the valleys of the Matrosskaya River (on the eastern slope of Vernadsky Ridge) and Pereturpit River (on the western slope of Vernadsky Ridge). Based on the geological data, a sublatitudinal trend has been established [4]. In the tectonic fragmentation model (see Figs. 4, 5a, 5c), this zone is most pronounced at depths of 0.5–1 km, and its width in some places is >2 km. The existence of a large fault here is evidenced by field observation data. The temperature in the middle part of the main channel of the Pereturpit River in August 2004 was 13.3°C, while the average monthly water temperature in surface streams on northern Paramushir during this period does not exceed 5–9°C. Such temperature values in the main river channel may indicate discharge of thermal waters in this area.

According to the latest data [20], an intrusive andesite body was discovered between the mouth areas of the Ptich'ya and Matrosskaya rivers. Probably, the identified intrusive body is associated with the emerging sill–dike complex of Mt. Mayak and Cape Krepkiy, the existence of which explains the vast zone of high rock fragmentation values in this sector.

On the western slope of Ebeko volcano is the Yur'eva River, the valley of which is oriented sublatitu-

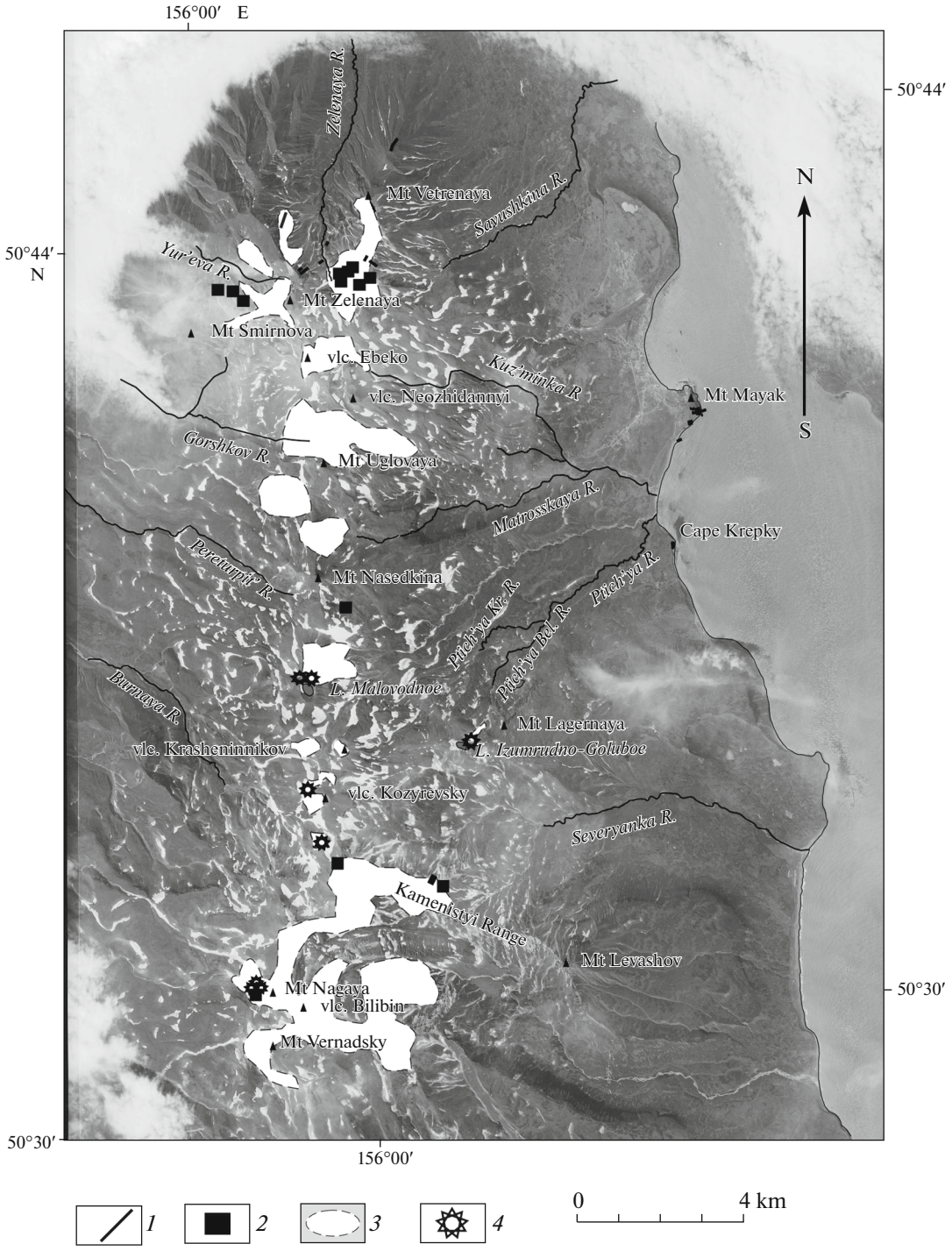

Fig. 6. Map of distribution zones of hydrothermally altered rocks (after [19] and authors' observations). (*1*) Dike; (*2*) neck; (*3*) distribution boundaries of hydrothermally altered rocks; (*4*) explosion funnels.

dinally. On the vertical section of the tectonic fragmentation model (see Fig. 5a) at a depth of 1000 m under the sources of the Yur'eva River, an anomalous zone for this area has been distinguished, with specific lengths of lineaments of 3.0 and 3.1. The zone coincides spatially with the subvolcanic intrusive body identified here [6], associated with the activity of the destroyed Vlodavets volcanic center. Hydrothermal activity manifests itself in the river valley in the height range from 280 to 560 m [26]. Mineral hot springs, in contrast to Ebeko volcano, are characterized by high-temperature (~87°C), ultra-acidic (pH 1–2) SO_4-Cl waters. The composition and temperatures are stable and do not change with the activ-

ity of Ebeko volcano [34]. The hydrothermal–magmatic system of the Yur'eva River valley is unique and daily supplies about 80 t of chlorine to the Sea of Okhotsk. After Yellowstone volcano in the United States and Domuyo volcano in Argentina, the sources of the Yur'eva River valley are the third largest in the world in terms of chlorine transport [46].

Clusters of anomalous rock fragmentation are observed along the entire eastern slope of Vernadsky Ridge (see Fig. 4). This zone is also well expressed on the map of the lineament network of northern Paramushir (see Fig. 2). Probably, there is a NNE-trending blind fault, which has been overprinted by numerous lava flows and therefore is poorly readable in the relief.

Our hypothesis is confirmed by a large number of discharges of cold and thermal groundwater sources onto the Earth's surface (see Fig. 2), an andesitic dikes and necks on Kamenisty Ridge (see Fig. 6), as well as Lake Izumrudno-Goluboe, and confined to a tectonic crush zone, the accumulation of explosion craters (see Fig. 6), concentrated along the intersection points of NNE-trending faults with the NW-trending faults.

In addition, a positive local gravity anomaly was revealed in the upper reaches of the Ptich'ya and Nasedkina rivers. In the opinion of the authors of [20], the anomaly is associated with a deep (2.5 km) intrusive body with mafic or intermediate composition emplaced in the fault zone. This is confirmed by high destruction here (see Fig. 5b), which formed above the intrusive bodies.

Comparing (1) the location of exposed intrusive bodies and explosion craters on Vernadsky Ridge (see Fig. 6), (2) the nature of volcanic activity and location of thermal water discharges, and (3) the created tectonic fragmentation model for northern Paramushir, it can be suggested that the heat supply of hydrothermal–magmatic systems came from small intrusive bodies (dikes, necks, etc.), concentrated in high tectonic fragmentation zones.

CONCLUSIONS

As a result of the study, on the basis of 3D modeling data of tectonic fragmentation, location of water discharge outlets, and analysis of volcanic activity on northern Paramushir Isl., the relationship between faults and the feeding of hydrothermal–magmatic systems was investigated.

(1) The dominant NE trend of faults has been established, with areal volcanism and hydrothermal–magmatic systems of Vernadsky Ridge. Ebeko volcano, which differs from other volcanoes in the productivity, nature, and frequency of eruptions, is located at the intersection of NE- and sublatitudinally trending faults. The activity of Ebeko volcano during the historical observation period and periodic changes in the composition of thermal mineral waters are most likely associated with the emplacement of low-volume intrusive bodies, such as sills and dikes.

(2) The revealed relationship between tectonic fragmentation and hydrothermal–magmatic activity on northern Paramushir Isl. reflects a general compression setting in the region and fracturing in the northeastern direction.

(3) In the north of the Kuril Island arc, the location of monogenic cinder cones of Alaid volcano, the shape of the volcanic edifice of Ebeko volcano, and the Yur'eva River canyon emphasize the sublatitudinal trend of faults, which formed as a result of evolution of the Kuril back-arc basin.

FUNDING

Collection of field material was carried out at IVS FEB RAS (Petropavlovsk-Kamchatsky, Russia) in the framework of research on the topic: "Evolution of Modern Hydrothermal–Magmatic Ore-Forming Systems of the Kuril-Kamchatka Island Arc" (state registration number 01.2.00 106353).

The study was supported by a megagrant of the Ministry of Education and Science of the Russian Federation (no. 14.W03.31.0033).

REFERENCES

1. G. P. Avdeiko, A. Yu. Antonov, O. N. Volynets, and A. A. Tsvetkov, *Submarine Volcanism and Zonality of the Kuril Island Arc*, Ed. by Yu. M. Pushcharovskii (Nauka, Moscow, 1992) [in Russian].
2. G. P. Avdeiko, S. V. Popruzhenko, and A. A. Palueva, "The tectonic evolution and volcano-tectonic zonation of the Kuril-Kamchatka island-arc system," Geotectonics **36**, 312–327 (2002).
3. G. P. Avdeiko, D. P. Savel'ev, S. V. Popruzhenko, and A. A. Palueva, "The principle of actualism: Criteria for paleotectonic reconstructions as exemplified by the Kuril–Kamchatka region," Vestn. KRAUNTs. Ser. Nauki Zemle **1** (1) 32–59 (2003).
4. *Atlas of Kuril Islands*, Ed. by V. M. Kotlyakov, P. Ya. Baklanov, N. N. Komedchikov, and E. A. Fedorova (DIK, Moscow, 2009) [in Russian].
5. V. I. Belousov, *Geology of Geothermal Filed in the Regions of Modern Volcanism* (Nauka, Moscow, 1978) [in Russian].
6. V. A. Bernshtein, S. S. Sivozhelezov, V. I. Fedorchenko, and V. N. Shilov, "Geophysical observations at some volcanoes of the Vernadsky Range," in *Comprehensive Studies in the Areas of Modern and Recent Volcanism: Case Study of the Vernadsky Range, Paramushir Island*, Vol. 16 of *Tr. Sakhalin. Kompl. Nauchno-Issled. Inst.*, Ed. by S. I. Naboko (Yuzhno-Sakhalinsk, 1966), pp. 44–65.
7. O. V. Bergal-Kuvikas, "Peculiarities of the spatial variations of volcanism from the Paramushir group, Kuril Island Arc," Vestn. KRAUNTs. Ser. Nauki Zemle **20** (2) 194–207 (2012).

8. O. V. Bergal-Kuvikas, "Volumes of Quaternary volcanics of the Kuril Island Arc: Analysis spatial distribution and relationship to the subduction zone," Tikhookean. Geol. **34**, 103–116 (2015).
9. C. B. Bortnikova, E. P. Bessonova, L. B. Trofimova, T. A. Kotenko, and I. V. Nikolaeva, "Hydrogeochemistry of gas-hydrothermal sources of Ebeko volcano, Paramushir Island," Vulkanol. Seismol., No. 1, 39–51 (2006).
10. G. S. Gorshkov, *Volcanism of the Kuril Island Arc* (Nauka, Moscow, 1967) [in Russian].
11. A. B. Efimov and T. Ya. Ershova, "On thermomechanical regime of the system surrounding the magmatic conduit," Vulkanol. Seismol., Nos. 4–5, 88–102 (1998).
12. A. V. Zhuravlev, "Geological structures and evolution of the South Okhotsk (Kuril) Basin," in *Structure and Position of the Northwest Pacific Sedimentary Basin*, Ed. by I. K. Tuesov (Dal'nevost. Geol. Inst., Vladivostok, 1982), pp. 23–33.
13. Ya. G. Kats, A. I. Poletaev, and E. F. Rumyantseva, *Fundamentals of Lineament Tectonics* (Nedra, Moscow, 1986) [in Russian].
14. T. A. Kotenko, L. V. Kotenko, E. I. Sandimirova, V. N. Shapar', and I. F. Timofeeva, "Eruptive activity of Ebeko volcano, Paramushir Island, in 2010–2011," Vestn. KRAUNTs. Ser. Nauki Zemle **19** (1), 160–167 (2012).
15. E. K. Markhinin and S. S. Sidorov, "Systematic description of hydrothermal manifestations at Ebeko and Vlodavets volcanoes in 1959–1960," in *Comprehensive Studies in the Areas of Modern and Recent Volcanism: Case Study of the Vernadsky Range, Paramushir Island*, Vol. 16 of *Tr. Sakhalin. Kompl. Nauchno-Issled. Inst.*, Ed. by S. I. Naboko (Yuzhno-Sakhalinsk, 1966), pp. 135–147.
16. I. V. Melekestsev, V. N. Dvigalo, V. Yu. Kir'yanov, A. V. Kurbatov, and I. A. Nesmachnyi, "Ebeko volcano (Kuril Islands): History of eruptive activity and future volcanic hazard. Pt. I," Vulkanol. Seismol., No. 3, 69–81 (1993).
17. I. V. Melekestsev, V. N. Dvigalo, V. Yu. Kir'yanov, A. V. Kurbatov, and I. A. Nesmachnyi, "Ebeko volcano (Kuril Islands): History of eruptive activity and future volcanic hazard. Pt. II," Vulkanol. Seismol., No. 4, 24–42 (1993).
18. Yu. V. Nechaev, *Lineaments and Tectonic Partitioning: Remote Studies of the Inner Structure of the Lithosphere* (Inst. Fiz. Zemli Ross. Akad. Nauk, Moscow, 2010) [in Russian].
19. *Recent and Modern Volcanism in the Territory of Russia*, Ed. by N. P. Laverov (Nauka, Moscow, 2005) [in Russian].
20. V. E. Podoshvin, *Study of Vapor Hydrotherms at the High-Scarp and Near-Mouth Sites of the North Paramushir Hydrothermal System* (MP-Elektra, Yuzhno-Sakhalinsk, 2012) [in Russian].
21. K. F. Sergeev, *Tectonics of the Kuril Island System* (Nauka, Moscow, 1976) [in Russian].
22. M. D. Sidorov and V. V. Taskin, "Voxel model of crustal fragmentation in the areas of hydrothermal deposits (Kamchatka)," Gorn. Inf.-Anal. Byull., Spec. No. S32, 336–341 (2017).
23. V. V. Taskin, "Brief review of foreign geological applications of the lineament analysis," Gorn. Inf.-Anal. Byull., Spec. No. S32, 138–144 (2017).
24. V. V. Taskin and M. D. Sidorov, "Algorithm of making a three-dimensional model of tectonic fragmentation in the GIS environment based on the results of deciphering aerial and satellite images; assessment of this model reliability," Geoinformatika, No. 1, 21–27 (2015).
25. V. V. Taskin and M. D. Sidorov, "A three-dimensional model of tectonic fragmentation of the Earth's crust, made using satellite video information," Sovrem. Probl. Distantsionnogo Zondirovaniya Zemli Kosmosa **11**, 243–252 (2014).
26. S. M. Fazlullin, "Geochemical system of the Yur'eva River (Kuril Islands): Conditions of chemical elements supply into and removal from the river basin," Vulkanol. Seismol., No. 1. 54–67 (1999).
27. V. I. Fedorchenko, A. I. Abdurakhmanov, and R. I. Rodionova, *Volcanism of the Kuril Island Arc: Geology and Petrogenesis* (Nauka, Moscow, 1989) [in Russian].
28. G. G. Khramova, *Formation Dynamics of Crater-Lake Sediments: Case Study of Ebeko Volcano* (Dal'nevost. Otd. Akad. Nauk SSSR, Vladivostok, 1987) [in Russian].
29. O. R. Khubaeva, G. V. Bryantseva, and L. A. Sim, "Recent deformations of the northern Paramushir Island," *Proceedings of the XI Meeting on Tectonics "Fundamental Problems of Geotectonics," Moscow, Russia, 2007* (GEOS, Moscow, 2007), Vol. 1, pp. 109–111.
30. B. V. Baranov, R. Werner, K. A. Hoernle, I. B. Tsoy, P. van den Bogaar, and I. A. Tararin, "Evidence for compressionally induced high subsidence rates in the Kurile Basin (Okhotsk Sea)," Tectonophysics **350**, 63–97 (2002).
31. B. Baranov, H. K. Wong, K. Dozorova, B. Karp, T. Lüdmann, and V. Karnaukh, "Opening geometry of the Kurile Basin (Okhotsk Sea) as inferred from structural data," Island Arc **11**, 206–219 (2002).
32. O. Bergal-Kuvikas, PhD Thesis (Hokkaido, 2015).
33. A. Gudmundsson, "Infrastructure and mechanics of volcanic systems in Iceland," J. Volcanol. Geotherm. Res. **64**, l–22 (1995).
34. E. Kalacheva, Y. Taran, T. Kotenko, K. Hattori, L. Kotenko, and G. Solis-Pichardo, "Volcano–hydrothermal system of Ebeko volcano, Paramushir, Kuril Islands: Geochemistry and solute fluxes of magmatic chlorine and sulfur," J. Volcanol. Geotherm. Res. **310**, 118–131 (2016).
35. A. V. Kiryukhin, A. Y. Polyakov, and O. O. Usacheva, "Thermal-permeability structure and recharge conditions of the Mutnovsky high-temperature geothermal field (Kamchatka, Russia)," J. Volcanol. Geotherm. Res. **356**, 36–55 (2018).
36. A. M. F. Lagmay and W. Valdivia, "Regional stress influence on the opening direction of crater amphitheaters in Southeast Asian volcanoes," J. Volcanol. Geotherm. Res. **158**, 139–150 (2006).
37. N. Le Corvec, K. B. Spörli, J. Rowland, and J. Lindsay, "Spatial distribution and alignments of volcanic

centers: clues to the formation of monogenetic volcanic fields," Earth Sci. Rev. **124**, 96–114 (2013).

38. I. Moriya, "Bandaian eruption and landform associated with it," in *Collection of Articles in Memory of Retirement of Prof. K. Nishimura* (Tohoku Univ., Sendai, 1980), pp. 214–219.
39. I. A. Menyailov, L. P. Nikitina, and V. N. Shapar, "Results of geochemical monitoring of the activity of Ebeko volcano (Kurile Islands) used for eruption prediction," J. Geodyn. **3**, 259–274 (1985).
40. K. Nakamura, "Volcanoes as possible indicators of tectonic stress orientation principle and proposal," J. Volcanol. Geotherm. Res. **2**, 1–16 (1977).
41. K. Nakamura and S. Uyeda, "Stress gradient in arc-back arc regions and plate subduction," J. Geophys. Res., B **85**, 6419–6428 (1980).
42. D. L. Nielson, J. W. Shervais, and J. Glen, "Conceptual model for a basalts-related geothermal system Mountain Home AFB, Idaho, USA," *44th Workshop on Geothermal Reservoir Engineering, Stanford, Calif. California, 2019*, pp. 1–4.
43. L. Siebert, "Large volcanic debris avalanches: characteristics of source areas, deposits, and associated eruptions," J. Volcanol. Geotherm. Res. **22**, 163–197 (1984).
44. M. D. Sidorov and V. V. Taskin, "The study of the permeability of the upper crust part on the photo image of the surface in the area of the Nalychevo field of thermomineral waters (Kamchatka)," *2nd International Geothermal Conference "GEOHEAT2018," Petropavlovsk-Kamchatsky, Russia, 2018*, pp. 1–10.
45. Y. Taran, M. Zelenski, I. Chaplygin, N. Malik, R. Campion, S. Inguaggiato, and T. Fischer, "Gas emissions from volcanoes of the Kuril island arc (NW pacific): Geochemistry and fluxes," Geochem. Geophys. Geosyst. **19**, 1859–1880 (2018).
46. Y. Taran and E. Kalacheva, "Role of hydrothermal flux in the volatile budget of a subduction zone: Kuril arc, Northwest Pacific," Geology **47**, 87–90 (2019).
47. A. Tibaldi, "Morphology of pyroclastic cones and tectonics," J. Geophys. Res.: Solid Earth. **100**, 24521–24535 (1995).
48. ArcGIS Desktop. https://www.esri.com/. Accessed April 25, 2014.
49. Geosoft Software, Oasis montaj. http://www.geosoft.com/ru/. Accessed November 12, 2009.
50. United States Geological Survey. https://www.usgs.gov/. Accessed April 1, 2019.